Lei O. Li,[1] Trisha J. Grevengoed,[1] David S. Paul,[1] Olga Ilkayeva,[2] Timothy R. Koves,[2] Florencia Pascual,[1] Christopher B. Newgard,[2] Deborah M. Muoio,[2] and Rosalind A. Coleman[1]

Compartmentalized Acyl-CoA Metabolism in Skeletal Muscle Regulates Systemic Glucose Homeostasis

Diabetes 2015;64:23–35 | DOI: 10.2337/db13-1070

The impaired capacity of skeletal muscle to switch between the oxidation of fatty acid (FA) and glucose is linked to disordered metabolic homeostasis. To understand how muscle FA oxidation affects systemic glucose, we studied mice with a skeletal muscle–specific deficiency of long-chain acyl-CoA synthetase (ACSL)1. ACSL1 deficiency caused a 91% loss of ACSL-specific activity and a 60–85% decrease in muscle FA oxidation. *Acsl1*$^{M-/-}$ mice were more insulin sensitive, and, during an overnight fast, their respiratory exchange ratio was higher, indicating greater glucose use. During endurance exercise, *Acsl1*$^{M-/-}$ mice ran only 48% as far as controls. At the time that *Acsl1*$^{M-/-}$ mice were exhausted but control mice continued to run, liver and muscle glycogen and triacylglycerol stores were similar in both genotypes; however, plasma glucose concentrations in *Acsl1*$^{M-/-}$ mice were ~40 mg/dL, whereas glucose concentrations in controls were ~90 mg/dL. Excess use of glucose and the likely use of amino acids for fuel within muscle depleted glucose reserves and diminished substrate availability for hepatic gluconeogenesis. Surprisingly, the content of muscle acyl-CoA at exhaustion was markedly elevated, indicating that acyl-CoAs synthesized by other ACSL isoforms were not available for β-oxidation. This compartmentalization of acyl-CoAs resulted in both an excessive glucose requirement and severely compromised systemic glucose homeostasis.

Skeletal muscle switches between the use of glucose and lipid, depending on fuel availability and energy requirements. Metabolic inflexibility, a state of impaired capacity for fuel switching between fatty acids (FAs) and glucose (1), is associated with metabolic disorders such as insulin resistance, diabetes, and the cardiometabolic syndrome (2–5), whereas enhanced oxidation of FA spares glucose (6,7). Metabolic inflexibility occurs in human disorders in which β-oxidation is genetically impaired; these disorders are associated with hepatic steatosis, myopathy, cardiomyopathy, and episodes of fasting-induced nonketotic hypoglycemia (8). However, it remains uncertain how fuel selection is regulated in skeletal muscle and how fuel inflexibility specifically impairs exercise tolerance and leads to metabolic dysfunction (7,9).

Before FAs are used for oxidation or for the synthesis of cholesterol esters, phospholipids, or triacylglycerol (TAG), they must be activated to form acyl-CoAs by one of a family of five long-chain acyl-CoA synthetases (ACSLs), each encoded by a separate gene (10). We have proposed that each ACSL isoform determines whether FAs are channeled toward pathways of oxidation or complex lipid biosynthesis (11). Data from ACSL1 deficiencies in adipose, liver, heart, or macrophages suggest that channeling is tissue-specific, but that in highly oxidative tissues, the ACSL1 isoform directs FAs toward β-oxidation (11–14). Thus, mice deficient in brown adipose ACSL1 cannot metabolize FAs for heat production and fail to maintain a normal body temperature when placed in a cold environment (13). Likewise, hearts that lack ACSL1 cannot oxidize FAs for contractile energy, have an eightfold increased use of glucose, and develop mammalian target of rapamycin complex 1–mediated hypertrophy (14).

[1]Department of Nutrition, University of North Carolina, Chapel Hill, NC
[2]Sarah W. Stedman Nutrition and Metabolism Center, and Departments of Medicine and Pharmacology and Cancer Biology, Duke University, Durham, NC
Corresponding author: Rosalind A. Coleman, rcoleman@unc.edu.

Received 8 July 2013 and accepted 23 July 2014.

This article contains Supplementary Data online at http://diabetes.diabetesjournals.org/lookup/suppl/doi:10.2337/db13-1070/-/DC1.

© 2015 by the American Diabetes Association. Readers may use this article as long as the work is properly cited, the use is educational and not for profit, and the work is not altered.

ACSL1 is located on the mitochondrial outer membrane, but it is unclear why its absence would block FA oxidation; acyl-CoAs are amphipathic molecules that are both soluble in water and able to integrate into membrane monolayers via their hydrophobic acyl chains. In addition, acyl-CoA binding protein and some isoforms of FA binding protein can bind and carry acyl-CoAs. Thus, an acyl-CoA should be able to enter any downstream pathway, unless the entry into one specific pathway versus another depend on the relative substrate affinities of the initiating acyltransferases.

The role of any ACSL isoform in skeletal muscle remains unknown (6,15). Given the importance of lipid metabolism in skeletal muscle and the key position of ACSL in initiating most lipid metabolic pathways, we hypothesized that a deficiency of ACSL1 would block the use of FAs for energy, thereby impairing fuel selection during exercise. To learn whether ACSL1 deficiency in skeletal muscle impairs exercise capacity or alters whole-body fuel metabolism, we studied the metabolic adaptation of skeletal muscle–specific *Acsl1* knockout mice ($Acsl1^{M-/-}$) to physiological challenges. Unexpectedly, acyl-CoA content rose markedly during exercise, revealing that acyl-CoAs synthesized by non-ACSL1 isoforms were retained in a pool that was inaccessible for mitochondrial oxidation.

RESEARCH DESIGN AND METHODS

Muscle-Specific *Acsl1* Knockout Mice

Homozygous floxed mice ($Acsl1^{loxP/loxP}$) (12) were mated with mice expressing Cre recombinase controlled by the muscle-specific human skeletal actin (HSA) promoter (catalog #006149; The Jackson Laboratory) to achieve muscle-specific deletion of *Acsl1*. HSA-Cre is expressed in the early embryo (16), and mice were born with deficient ACSL1. $Acsl1^{M-/-}$ ($Acsl1^{loxP/loxP}$-*HSACre*) were mated with $Acsl1^{loxP/loxP}$ mice to obtain $Acsl1^{M-/-}$ and littermate controls ($Acsl1^{loxP/loxP}$). Because most measurements were qualitatively similar in male and female $Acsl1^{M-/-}$ mice compared with controls, we report measurements from only one sex. Procedures were approved by the University of North Carolina Institutional Animal Care and Use Committee. Mice were kept in a pathogen-free barrier facility (12-h dark/light cycle) and fed standard chow (Prolab RMH 3000; LabDiet, Richmond, IN). Between 8 and 25 weeks of age, some mice were fed a high-fat diet (45%; D12451) or a matched low-fat (10%; D12450B) standard diet (Research Diets). Oral glucose (2.5 g D-glucose/kg body wt) and intraperitoneal insulin tolerance tests (control diet 0.35 units/kg body wt; high-fat diet 0.50 units/kg body wt) (12) and glycerol tolerance tests (2 mg/kg body wt) (17) were performed.

Metabolic analysis was performed in PhenoMaster/LabMaster chambers (TSE Systems, Chesterfield, MO). After 24 h of acclimatization, measurements were acquired every 27 min for V_{O_2}, V_{CO_2}, respiratory exchange ratio (RER), food intake, and physical activity.

Endurance Exercise

Mice (16–26 weeks of age) were acclimatized to a motorized, speed–controlled treadmill with an electric shock stimulus (Exer-3/6; Columbus Instruments, Columbus, OH) for 3 consecutive days, starting from 0 to 16 m/min and from 0 to 10% grade. On the study day, mice were fasted for 2 h after 10:00 A.M. ("rested" state) to prevent potential carbohydrate-induced increases in insulin with a subsequent decrease in adipose lipolysis (18). Speed was increased from 8 m/min by 2 m/min every 15 min until reaching 18 m/min. Mice were maintained at this speed until they refused to run. Tail blood was taken for measurement of glucose and lactate levels. For measurement of plasma metabolites and tissue glycogen, trunk blood and tissues were collected at exhaustion. Blood and tissues were taken from additional control mice after they had run for the same length of time as the exhausted $Acsl1^{M-/-}$ mice.

Metabolites, Western Blot Analysis, and Histology

Mice were fasted for 4 h (basal state) or 17 h. Plasma metabolites were measured colorimetrically (glucose, nonesterified FA; Wako, Richmond, VA; triglyceride; Stanbio Laboratory, Elkhart, IN) or enzymatically (β-hydroxybutyrate, creatine kinase; Stanbio Laboratory), with a mouse insulin ELISA kit (Millipore, Billerica, MA) or with a lactometer (Lactate Plus; Nova Biomedical, Waltham, MA). Glycogen was measured in snap-frozen tissues (19). TAG was measured in tissue lipid extracts (Stanbio Laboratory) (20,21). Gastrocnemius muscle was fixed and stained (22).

Tissue proteins were blotted with primary antibodies to detect ACSL1, Akt, and pAkt (Cell Signaling Technology, Danvers, MA); ACSL4 (Santa Cruz Biotechnology, Santa Cruz, CA); and GLUT1 and GAPDH (Abcam, Cambridge, MA).

Insulin Signaling

Mice were injected with PBS or insulin (2 units/kg body wt i.p.). Glucose was measured by glucometer to ensure adequate lowering. Ten minutes later, tissue supernatants were prepared, electrophoresed, and blotted for antiphospho-Akt (Thr-308) and total Akt (Cell Signaling Technology) (20).

Quantitative PCR

Genomic/mitochondrial DNA and total RNA were extracted from tissues (TRIzol; Invitrogen, Carlsbad, CA; AllPrep DNA/RNA kit; Qiagen, Valencia, CA). cDNA was synthesized (Applied Biosystems). Gene expression and mitochondrial DNA content were determined with Absolute QPCR Sybr Green Fluorescein Mix (Thermo Scientific, West Palm Beach, FL). Expression of target genes (Supplementary Table 1) was normalized to endogenous β-actin, tubulin, or H19 and calculated using the $2^{-\Delta\Delta Ct}$ method (23).

ACSL Activity, FA Oxidation, and Metabolomics

ACSL-specific activity was measured in tissue homogenates from 13- to 16-week-old mice (24). CO_2 and acid soluble metabolites (ASM) were measured from gastrocnemius

homogenates incubated for 30 min in 100 mmol/L KCl, 40 mmol/L Tris-HCl, 10 mmol/L Tris base, 5 mmol/L $MgCl_2 \cdot 6H_2O$, 1 mmol/L EDTA, and 1 mmol/L ATP, pH 7.4, and [1-^{14}C]palmitate or [1-^{14}C]palmitoyl-CoA (25). Amino acids, acyl-carnitines, acyl-CoAs, and ceramides were analyzed by flow injection tandem mass spectrometry (26,27). Organic acids were analyzed by gas chromatography–mass spectrometry (27).

For whole-muscle incubations, soleus and extensor digitorum longus muscles were removed (fed state) and incubated (28) with gassing in Krebs-Henseleit buffer, 5 mmol/L D-glucose, 1 mmol/L L-carnitine, 12.5 mmol/L HEPES, and 1% BSA. Media were changed after 30 min. Contralateral muscles were incubated with 1 mmol/L [1-^{14}C]oleate (2 μCi/ml) or with 5 mmol/L [U-^{14}C]glucose (2 μCi/ml), 100 nmol/L insulin, and 0.75 mmol/L palmitate for 90 min. Media were transferred to culture tubes containing 1 N NaOH CO_2 traps. $^{14}CO_2$ and [^{14}C]ASM were assessed (28).

Statistics

Data were analyzed using a two-tailed Student *t* test or two-way ANOVA where appropriate (SAS, Inc.) and were expressed as means ± SE. Statistical significance was defined as $P < 0.05$.

RESULTS

FA Oxidation Was Severely Diminished in *Acsl1*$^{M-/-}$ Skeletal Muscle

In *Acsl1*$^{M-/-}$ mice, weight and activity did not differ from those in littermate controls, and female reproduction was normal. ACSL1 protein was absent in *Acsl1*$^{M-/-}$ gastrocnemius muscle but was present in the heart (Fig. 1*A*) and liver (Supplementary Fig. 1*A*). *Acsl1* mRNA expression in gastrocnemius muscle was 86% lower than that in controls, with no compensatory increases in other ACSL isoforms (Fig. 1*B*). Compared with controls, the mRNA content of *Acsl4* was 30% lower in *Acsl1*$^{M-/-}$ gastrocnemius muscle and 35% higher in soleus muscle (Supplementary Fig. 1*B*), but ACSL4 gastrocnemius muscle protein content was unchanged (Supplementary Fig. 1*C*). ACSL-specific activity was unchanged in the heart but was diminished by >90% in *Acsl1*$^{M-/-}$ gastrocnemius muscle (Fig. 1*C*). Residual ACSL activity represents the combined activities of all remaining ACSL isoforms. These data show that ACSL1 contributes the majority of total ACSL activity in skeletal muscle.

Deficiency of ACSL1 caused a mild myopathy with occasional central nuclei and cells surrounded by macrophages (Fig. 1*D* and *E*), but plasma creatine kinase activity was not statistically elevated (Table 1). Compared with controls, the sum of complete oxidation of [1-^{14}C]palmitate to CO_2 plus incomplete oxidation to ASM was 83% and 63% lower, respectively, in *Acsl1*$^{M-/-}$ gastrocnemius and soleus muscles (Fig. 1*F*). Unimpaired oxidation of [^{14}C]palmitoyl-CoA to CO_2 (Fig. 1*G*) and the presence of normal mitochondrial DNA content (Supplementary Fig. 1*D*) indicated that ACSL1 deficiency did not block the downstream FA oxidation pathway or diminish mitochondrial respiratory function. The significant decrease in FA oxidation in *Acsl1*$^{M-/-}$ muscle suggests that the ACSL1 isoform is required to activate FAs before they can be converted to acyl-carnitines, enter the mitochondrial matrix, and undergo β-oxidation; in contrast, acyl-CoAs were oxidized.

Because the preparation of homogenates or isolated mitochondria alters normal organelle relationships, we performed additional studies in permeabilized muscle fibers. FA oxidation in permeabilized fibers was only 1% of the oxidation in homogenates (compare Fig. 1*F* and *H*), and neither glucose nor FA oxidation or FA incorporation into complex lipids was impaired (Fig. 1*I* and *J*), suggesting that maximal FA transport, similar to that of glucose, may require specific transporters or ACSL isoforms that are activated by muscle contraction. Experiments using homogenates or isolated mitochondria would eliminate the transport step and permit ACSL1 to directly activate FAs and allow them to be converted to acyl-carnitines for mitochondrial entry. Alternatively, in static muscle, perhaps only very small amounts of FA enter the mitochondria for oxidation, and these small amounts of acyl-CoAs are supplied by non–ACSL1 isoforms such as ACSL5, which is also present on the outer mitochondrial membrane (10).

ACSL1 Deficiency in Muscle Impairs Fasting Glucose Homeostasis

To examine how the limitation in skeletal muscle FA oxidation affects whole-body energy metabolism, we challenged *Acsl1*$^{M-/-}$ mice with an overnight fast, a state in which FAs released from adipose become the major fuel source for most organs. *Acsl1*$^{M-/-}$ mice became mildly hypoglycemic (plasma glucose level: 82 ± 6 mg/dL vs. 137 ± 24 mg/dL in controls) (Fig. 2*A*). Compared with controls, basal plasma FA concentrations were 64% higher in *Acsl1*$^{M-/-}$ mice and rose further after an overnight fast (0.58 ± 0.04 vs. 0.25 ± 0.05 mmol/L, respectively) (Fig. 2*B*). After fasting, the plasma TAG level was 46% higher in *Acsl1*$^{M-/-}$ mice (Fig. 2*C*), and the plasma β-hydroxybutyrate level was 71% higher (Fig. 2*D*), consistent with increased hepatic β-oxidation of FA. Compared with fasting controls, fasting *Acsl1*$^{M-/-}$ mice stored 53% more TAG in the liver (Fig. 2*E* and *F*), suggesting that the inability of *Acsl1*$^{M-/-}$ muscle to metabolize FA caused adipose-derived FAs to relocate to the liver for re-esterification and storage (29,30).

Overnight fasting depleted liver glycogen stores in both control and knockout mice (Fig. 2*G*). Although mRNA abundance of glucose-6-phophatase and phosphoenolpyruvate carboxykinase increased similarly in both genotypes (Fig. 2*H*), which is consistent with appropriate gluconeogenic upregulation, this upregulation was insufficient to counteract hypoglycemia in *Acsl1*$^{M-/-}$ mice, probably because of diminished substrate availability since a glycerol tolerance test showed enhanced gluconeogenesis (Fig. 2*I*). The gastrocnemius muscle of *Acsl1*$^{M-/-}$ mice contained more GLUT1 protein (Fig. 2*J*). Weight

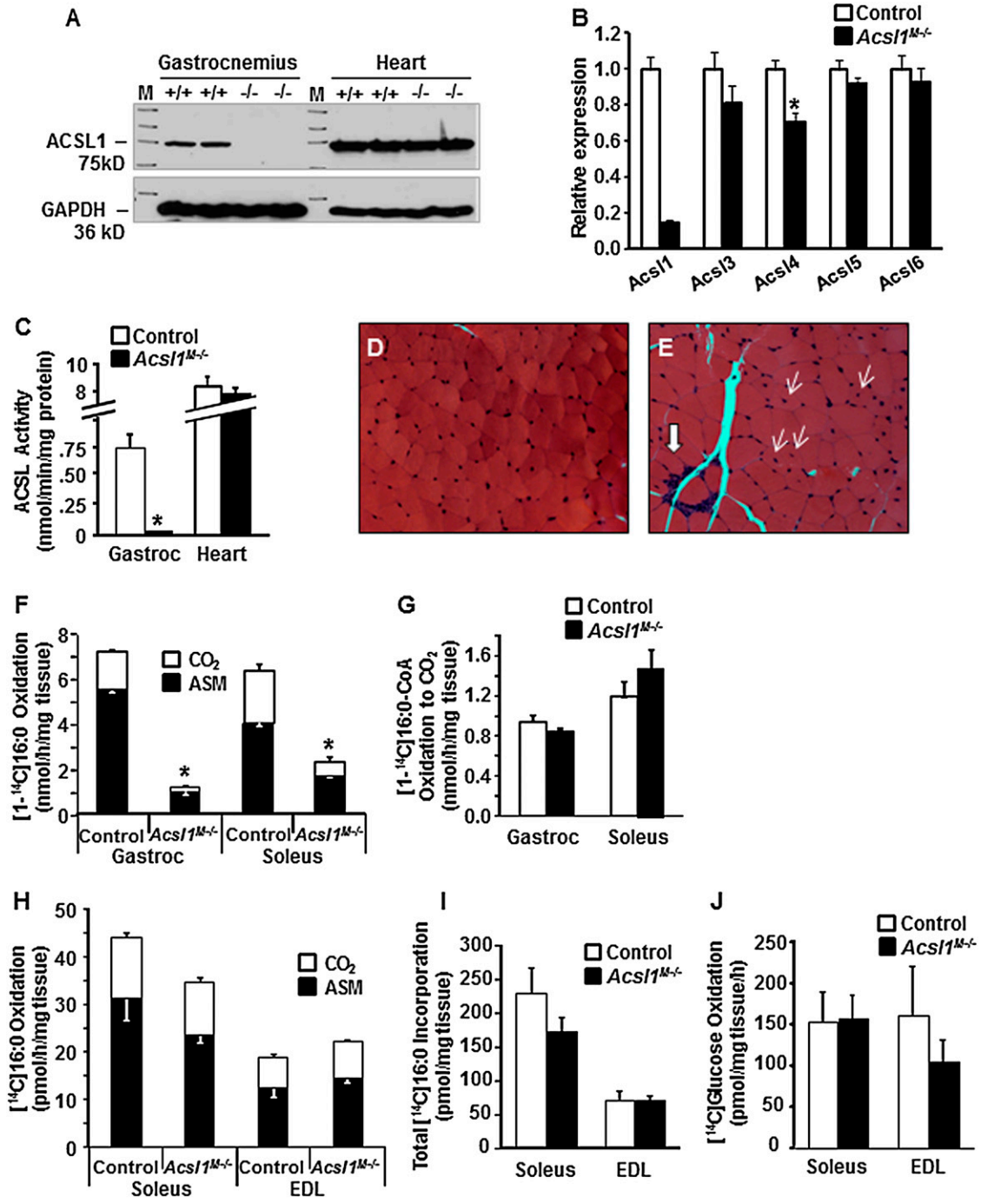

Figure 1—ACSL1 deficiency decreased ACSL-specific activity and FA oxidation in skeletal muscle. *A*: ACSL1 protein in the gastrocnemius muscle and heart in *Acsl1*$^{M-/-}$ and control mice. *B*: mRNA expression of *Acsl1* isoforms in gastrocnemius relative to tubulin (males; $n = 8$). *C*: ACSL-specific activity in homogenates from the gastrocnemius muscle and heart ($n = 4$). Histology (×20) of control (*D*) and *Acsl1*$^{M-/-}$ (*E*) gastrocnemius. Thin arrows, central nuclei; thick arrow, macrophage infiltration. FA oxidation in homogenates from gastrocnemius and soleus muscle from [1-^{14}C]palmitate (*F*) or [^{14}C]palmitoyl-CoA (*G*) ($n = 3$–4). Oxidation (*H*) or incorporation (*I*) in isolated soleus or extensor digitorum longus with [^{14}C]16:0, or with [^{14}C]glucose (*J*) ($n = 5$). *$P < 0.05$, compared with control littermates. EDL, extensor digitorum longus; Gastroc, gastrocnemius.

gain, body composition (Supplementary Fig. 2), and glucose tolerance test results showed no genotype differences in mice fed control or high-fat diets (Fig. 2*K*), but less insulin was secreted by *Acsl1*$^{M-/-}$ mice (Fig. 2*L*). Enhanced insulin sensitivity was confirmed by insulin tolerance tests (Fig. 2*M*), high basal pAkt (T308) levels in the liver, and increased pAkt levels in the liver and gastrocnemius muscle after insulin injection (Fig. 2*N*). Taken together, these data show that, during fasting, the inability of *Acsl1*$^{M-/-}$ skeletal muscle to switch from

Table 1—Metabolic parameters of *Acsl1*$^{M-/-}$ mice before and during endurance exercise

Metabolic parameters	Resting control mice (n = 4–6)	Resting *Acsl1*$^{M-/-}$ mice (n = 6–11)	Running control mice (n = 5)	Exhausted control mice (n = 6–7)	Exhausted *Acsl1*$^{M-/-}$ mice (n = 6–13)
Plasma					
TAG (mg/dL)	38.0 ± 3.6	34.9 ± 2.9	75.6 ± 5.3	73.1 ± 4.4†	52.7 ± 3.9*†
NEFA (mmol/L)	0.17 ± 0.03	0.28 ± 0.04*		1.28 ± 0.02†	1.32 ± 0.10†
β-Hydroxybutyrate (mmol/L)	0.33 ± 0.03	0.35 ± 0.05		0.99 ± 0.20†	0.83 ± 0.06†
Creatine kinase (units/L/min)	134 ± 6	248 ± 11‡		2347 ± 376†	2325 ± 183†
Liver					
Glycogen (μmol/g wet wt)	62.2 ± 14.7	40.1 ± 12.5	8.79 ± 0.96	9.32 ± 1.52†	7.77 ± 0.52†
TAG (μg/mg wet wt)	15.7 ± 1.5	15.6 ± 2.1		36.9 ± 3.0†	22.4 ± 3.0*†
Muscle					
Glycogen (μmol/g wet wt)	13.7 ± 1.2	15.6 ± 1.3	BD	BD†	BD†
TAG (μg/mg wet wt)	4.34 ± 0.57	3.60 ± 0.35		2.65 ± 0.54†	2.70 ± 0.44

Data are represented as the mean ± SE. BD, below detectable concentration; NEFA, nonesterified FA; Resting, data before exercise and after 2 h without food; Running control, data from control mice at the time when their *Acsl1*$^{M-/-}$ littermates were exhausted. *$P < 0.05$, *Acsl1*$^{M-/-}$ compared with control littermates (same conditions). †$P < 0.05$, compared with resting state (same genotype). ‡$P = 0.53$.

glucose to FA use resulted in an overflow of FAs to plasma and liver, thereby increasing liver TAG and plasma VLDL levels, diminishing plasma glucose levels, and increasing insulin sensitivity.

Metabolic Inflexibility During Fasting

The RER (V_{CO_2}/V_{O_2}) was consistent with impaired fuel switching from glucose to FA oxidation in *Acsl1*$^{M-/-}$ muscle (Fig. 3*A*). The RER did not differ between genotypes when mice were fed chow (60% carbohydrate), suggesting that muscle FA oxidation may not be critical without exercise, but when food was removed, the responses of the two genotypes diverged. Whether or not food is available at the start of the dark cycle, the RER normally rises; this rise in RER occurred in both control and *Acsl1*$^{M-/-}$ mice (Fig. 3*B* and Supplementary Fig. 3). However, although fasting decreased the total RER during both the day and night cycles, at every point during the dark cycle the RER of the *Acsl1*$^{M-/-}$ mice remained higher than that of the controls, indicating increased systemic use of glucose by *Acsl1*$^{M-/-}$ mice, despite the fast (Fig. 3*A* and *B*). With refeeding, the RER rose similarly in both genotypes, and the amount of food eaten and heat produced were similar (Fig. 3*C* and *D*). These data indicate that during fasting when FA is normally the major fuel source, *Acsl1*$^{M-/-}$ mice relied predominantly on nonlipid fuels; this requirement was less prominent in the nonfasted state, primarily because exercise was minimal in both genotypes.

Acsl1$^{M-/-}$ Mice Were Exercise Intolerant

During endurance exercise, *Acsl1*$^{M-/-}$ mice ran only 46–48% of the distance run by controls (1,522 ± 122 vs. 3,175 ± 327 m) (Fig. 4*A* and Supplementary Fig. 4*A*). Blood lactate levels increased minimally (Fig. 4*B*), indicating that the aerobic threshold had not been exceeded, but both genotypes ceased to run when their blood glucose concentrations dropped to ~40 mg/dL (Fig. 4*C*). Although glucose concentrations declined more slowly in control mice, at exhaustion, liver and muscle glycogen levels were equally depleted in both genotypes, and both were similarly hypoglycemic (Table 1). At exhaustion, plasma creatine kinase levels were similar in both genotypes.

At the time point when *Acsl1*$^{M-/-}$ mice refused to run further, running control mice had blood glucose values of 87 ± 7 mg/dL, despite depleted liver glycogen levels and undetectable muscle glycogen levels (Table 1). Because the basal content of liver and muscle glycogen was similar in both genotypes (Fig. 2*G*) and since liver glycogen stores were almost totally absent in the running controls, it appeared that gluconeogenesis in control mice was sufficient to avoid severe hypoglycemia, but *Acsl1*$^{M-/-}$ mice, despite similar increases in the expression of hepatic gluconeogenic genes (Fig. 4*D*), were unable to produce enough glucose to compensate for the increased muscle demand.

During prolonged exercise, hydrolyzed adipose FA becomes a major fuel source for most tissues (31). Endurance exercise increased plasma nonesterified FA levels in both genotypes (Table 1). Although an increase in plasma FA level normally increases liver TAG content during exercise, *Acsl1*$^{M-/-}$ mice accumulated less hepatic TAG than did controls, probably because more FA was used for energy in the liver (Table 1). Similarly, although plasma TAG levels increased in both genotypes, there was less of an increase in the *Acsl1*$^{M-/-}$ mice (Table 1). Intramuscular TAG is believed to be a major fuel source in muscle during endurance exercise (32), and, at exhaustion, control muscle had lost twice as much TAG (Table 1), which is consistent with their ability to use lipid for energy.

Basal Muscle and Plasma Metabolites Differed in *Acsl1*$^{M-/-}$ and Control Mice

To understand how FA use differs in exercising muscle, we profiled plasma and muscle metabolites. Consistent with absent ACSL1 activity, resting *Acsl1*$^{M-/-}$ muscle contained lower levels of long-chain acyl-CoAs (Fig. 5*A* and Supplementary Fig. 4*A*). Compared with controls,

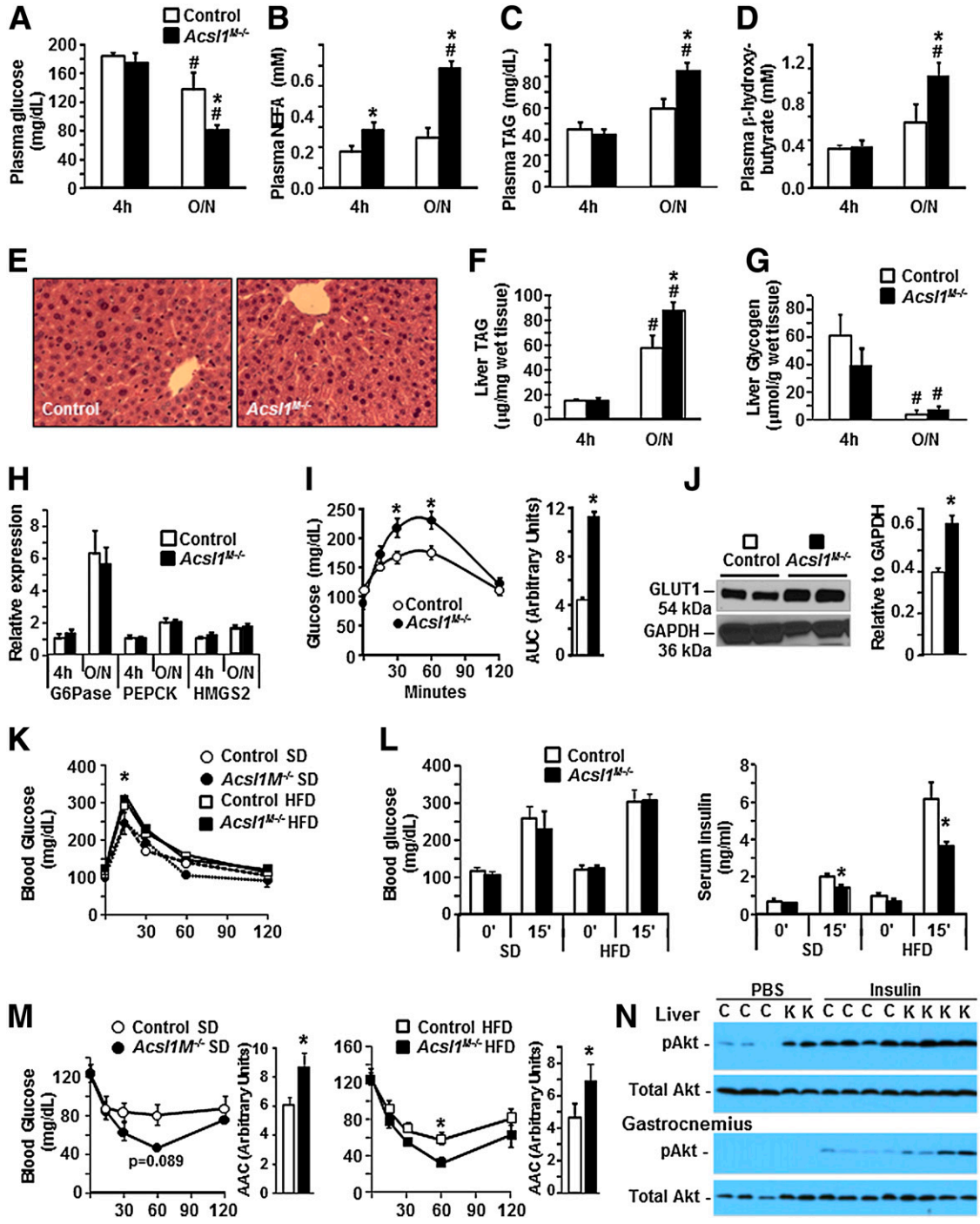

Figure 2—*Acsl1*$^{M-/-}$ mice were more vulnerable to hypoglycemia and hepatic lipid accumulation after an overnight fast and required less insulin to maintain euglycemia. Plasma glucose (*A*), nonesterified FAs (NEFAs) (*B*), TAG (*C*), and β-hydroxybutyrate (*D*) in female *Acsl1*$^{M-/-}$ after food removal for 4 h (n = 9–11) or fasting overnight (O/N) (n = 7–17). *E*: Histology of representative liver slides from female control and *Acsl1*$^{M-/-}$ mice after an overnight fast (hematoxylin-eosin staining). Measurement after an overnight fast of liver TAG (*F*) and glycogen (*G*) content (n = 4–8). *H*: Gene expression of glucose-6-phosphatase (G6Pase), phosphoenolpyruvate (PEPCK), and hydroxymethylglutaryl-CoA synthase-2 (HMGS2) in male mice (n = 6–10). *I*: Glycerol tolerance test in male mice after an overnight fast (n = 4). *J*: GLUT1 protein in gastrocnemius muscle (n = 4–5). In control and *Acsl1*$^{M-/-}$ female mice fed a high-fat diet (HFD) or matched standard diet (SD): glucose tolerance (*K*); blood glucose and insulin levels before and 15 min after intraperitoneal administration of insulin (*L*); and insulin tolerance tests and areas above the curve (AAC) after food removal for 4 h (*M*). *N*: pAkt (T308) and total Akt in female liver and gastrocnemius muscle 10 min after intraperitoneal PBS or insulin. C, control mice; K, knockout mice. #$P < 0.05$, vs. 4-h state (same genotype); *$P < 0.05$, vs. control (same treatment).

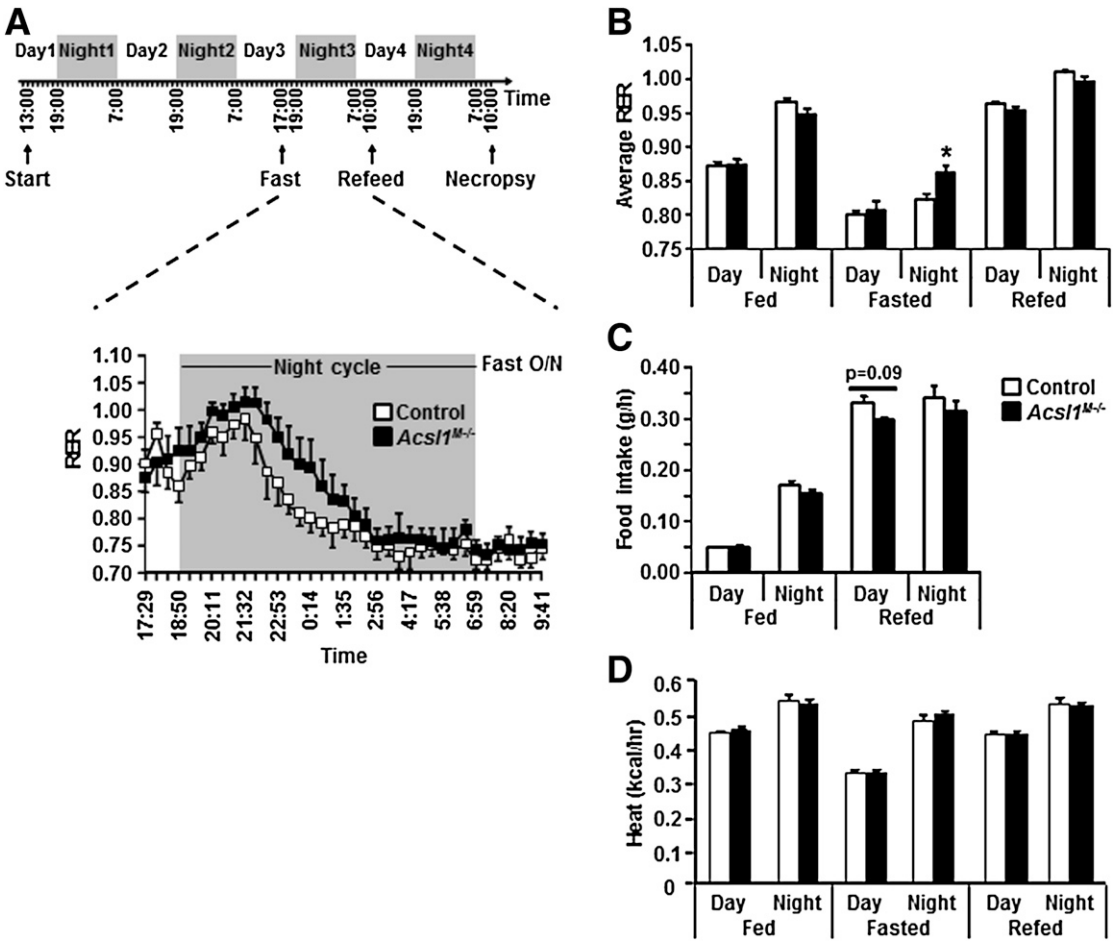

Figure 3—*Acsl1*$^{M-/-}$ mice used more glucose as fuel source. *A*: Male mice (13 wk) were placed in metabolic chambers at 1:00 P.M. and measurements were taken for 2 days before overnight (O/N; 5:00 P.M. to 10:00 A.M.) fasting. Mice were then refed with chow for 24 h (n = 4); RER (V_{CO_2}/V_{O_2}) was monitored by indirect calorimetry during O/N fasting. Average RER (*B*), food intake (*C*), and heat production (*D*) during day and night cycles when the mice were fed, fasted, or refed. *P < 0.05, compared with control.

acyl-CoA species of 14–18 carbons were 31–42% lower, but little difference was observed for short-chain acyl-CoAs, which are primarily products of amino acid degradation. Basal levels of long-chain acyl-carnitine species were similar in both genotypes (Fig. 5*B*). Acetyl-CoA is the final product of pathways of FA oxidation, glycolysis, and amino acid degradation. Basal acetyl-CoA levels were higher in *Acsl1*$^{M-/-}$ muscle than in that of controls (Fig. 5*A*). Because FA oxidation was severely impaired in *Acsl1*$^{M-/-}$ muscle and basal tricarboxylic acid (TCA) cycle intermediates were not limiting (Fig. 5*C*), this elevation in acetyl-CoA content, together with the lower basal content of total amino acids in *Acsl1*$^{M-/-}$ muscle, suggests an increase in the use of amino acids and glucose for energy, even without exercise (Fig. 5*D*). Levels of amino acids and acyl-carnitines in plasma did not differ between genotypes (Supplementary Fig. 5*B* and *C*).

Muscle and Plasma Metabolites Differed After Endurance Exercise

With endurance exercise, many acyl-CoA and acyl-carnitine metabolites increased markedly. In muscle from exhausted control mice, the levels of total acyl-CoA and long-chain acyl-CoA species each rose threefold (Fig. 5*A*), which is consistent with the normally enhanced influx of adipocyte-derived FA and its metabolism to acyl-CoA. Surprisingly, the increases of total acyl-CoA and long-chain acyl-CoA were even greater in *Acsl1*$^{M-/-}$ muscle than in that of controls, with 4- and 10-fold increases, respectively. Total long-chain acyl-CoA levels were 89% higher in exhausted knockout muscle than in exhausted control muscle, despite the absence of ACSL1, the 79% lower ACSL-specific activity, and the absence of increases in mRNA expression of other *Acsl* or *Fatp* isoforms (Fig. 6*A*) (33).

Acyl-carnitines, which normally correspond to acyl-CoA levels, differed greatly by genotype. Endurance exercise increased total and long-chain acyl-carnitines 5.5- and 23-fold, respectively, in control muscle, but only 3- and 12-fold, respectively, in *Acsl1*$^{M-/-}$ muscle. Thus, in exhausted *Acsl1*$^{M-/-}$ muscle, the levels of total and individual long-chain acyl-carnitine species were 33–77% lower than in exhausted controls, consistent with impaired FA oxidation (Fig. 5*B*), and levels of medium-chain

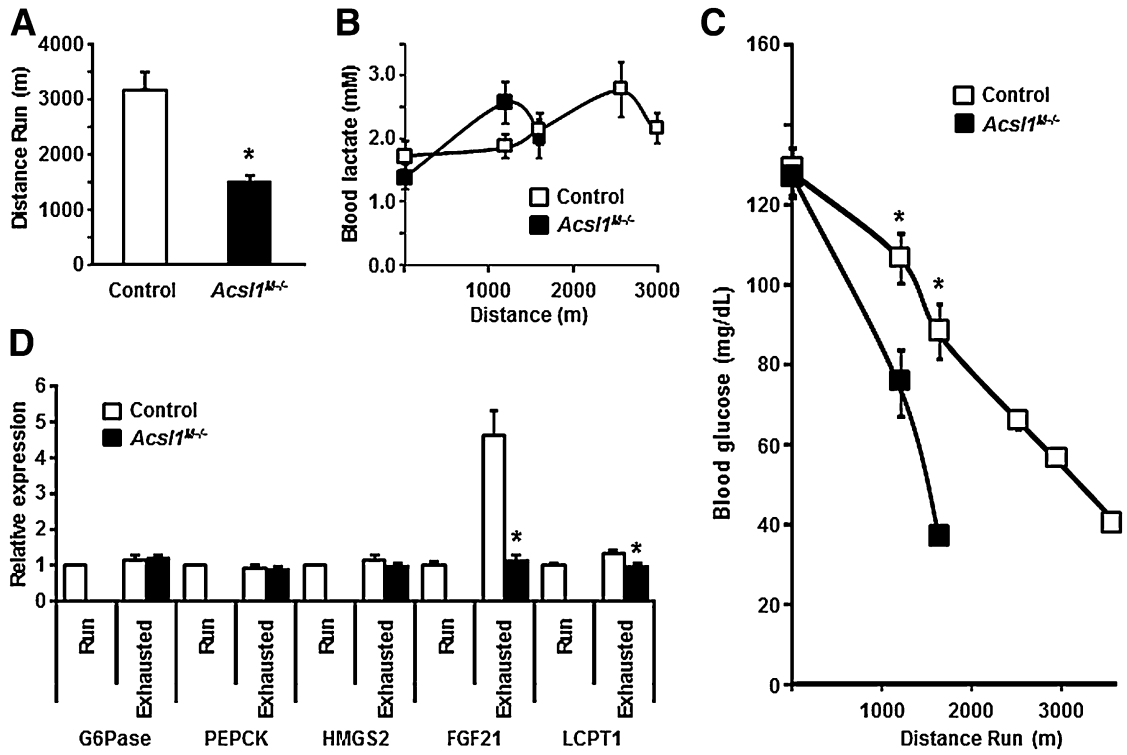

Figure 4—Muscle ACSL1 deficiency impaired endurance capacity. *A*: Total distance run during treadmill endurance exercise for $Acsl1^{M-/-}$ mice (16 weeks of age, female). Blood lactate (*B*) and glucose (*C*) levels during endurance exercise. *$P < 0.05$, glucose from exhausted $Acsl1^{M-/-}$ mice compared with control mice that had run same distance (Run). *D*: mRNA expression of glucose-6-phosphatase (G6Pase), phosphoenolpyruvate carboxykinase (PEPCK), FGF21, hydroxymethylglutaryl-CoA synthase-2 (HMGS2), and liver CPT1 (LCPT1) (n = 5–13). *$P < 0.05$, compared with exhausted controls. Run, data from control mice collected at the time their $Acsl1^{M-/-}$ littermates were exhausted.

acyl-carnitines were 30–77% lower than those in controls (Supplementary Fig. 5). These data indicate that, despite the marked decrease in skeletal muscle ACSL-specific activity in $Acsl1^{M-/-}$ mice, during endurance exercise plasma FAs taken up into muscle were converted to acyl-CoAs by other ACSL isoforms; these acyl-CoAs, however, remained in cytosolic pools that were inaccessible to carnitine palmitoyltransferase (CPT) 1 and β-oxidation enzymes in mitochondria and peroxisomes (34).

Exercise increases the demand for carnitine as a carrier for acyl groups (18). Although exercise diminished muscle carnitine content in both genotypes (Fig. 5*B*), free carnitine levels remained higher in $Acsl1^{M-/-}$ than in control muscle, both in the resting state and at exhaustion, indicating that the availability of carnitine had not limited the conversion of acyl-CoAs to acyl-carnitines. Because acyl-carnitines often reflect the flux of acyl-CoAs that enter the β-oxidation pathway, the observation that muscle from exhausted $Acsl1^{M-/-}$ mice contained higher amounts of long-chain acyl-CoAs but lower amounts of long-chain acyl-carnitines (Fig. 5*A* and *B*) strongly suggests that muscle contains separate pools of acyl-CoA. *Acsl3* mRNA was 40 and 30% higher, respectively, in resting and exhausted $Acsl1^{M-/-}$ muscle, but none of the other *Acsl* isoforms was specifically upregulated by exercise (Fig. 6*A*). In control muscle, the total specific activity derived from all ACSL isoforms was unchanged by exercise; however, in muscle from exhausted $Acsl1^{M-/-}$ mice, ACSL-specific activity more than doubled (0.06 ± 0.01 to 0.17 ± 0.04 nmol/min/mg protein), suggesting that one or more ACSL isoforms had been post-translationally activated by exercise (Fig. 6*B*). Lack of change in intramuscular TAG content in $Acsl1^{M-/-}$ mice (Table 1 and Fig. 6*C*) suggests that the accumulating long-chain-CoAs were not used for net TAG synthesis.

Intense exercise induces autophagy with the use of proteolyzed amino acids for both fuel within muscle and as a substrate for hepatic gluconeogenesis (35–37). With exercise, control muscle content of proline, valine, leucine/isoleucine, aspartate/asparagines, and tyrosine rose 57–115% (Fig. 5*D*); plasma branch-chain and aromatic amino acids increased two- to threefold (Supplementary Fig. 6*B*); and amino acid degradation products (short-chain C3–C6 acyl-carnitines) rose 3.5-fold (Supplementary Fig. 5*B*). In exhausted $Acsl1^{M-/-}$ muscle, however, the levels of proline, alanine, aspartate/asparagines, and the branched-chain amino acids were low (Fig. 5*D*), probably because these amino acids were diverted toward energy production within muscle, as indicated by the marked rise in short-chain acyl-CoA amino acid degradation products (Supplementary Fig. 5*A*). TCA intermediates were not depleted (Fig. 5*C*).

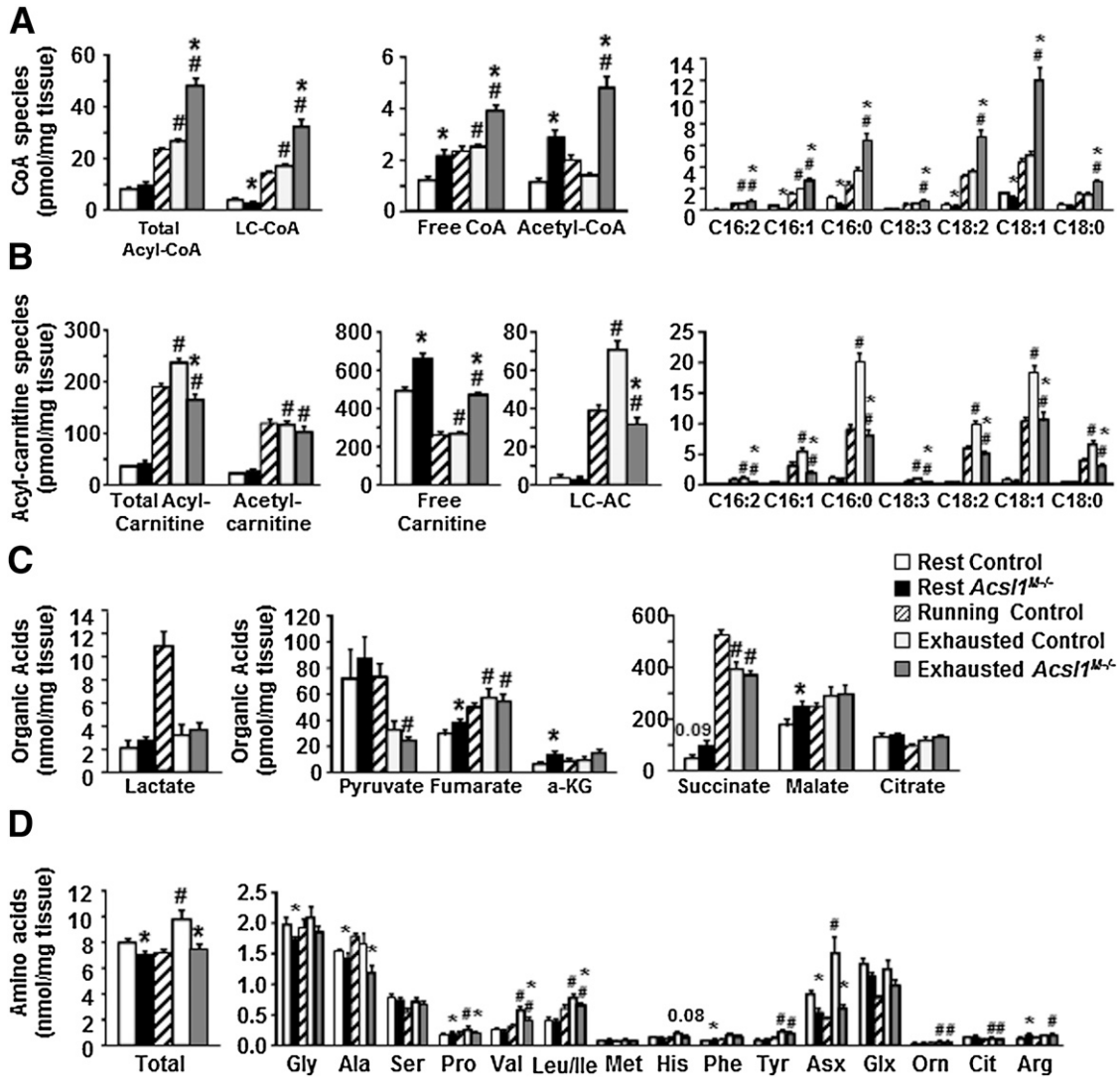

Figure 5—Metabolite changes in *Acsl1*$^{M-/-}$ gastrocnemius muscle during endurance exercise (16–26 weeks of age, female). *A*: Muscle free- and acyl-CoAs. *B*: Muscle free- and acyl-carnitines. *C*: Muscle Krebs cycle intermediates. *D*: Muscle amino acids (n = 5–9). #$P < 0.05$, vs. 4-h state (same genotype); *$P < 0.05$, vs. control (same treatment). Running, data from control mice collected when their *Acsl1*$^{M-/-}$ littermates were exhausted. a-KG, α-ketoglutarate; LC-AC, long-chain acyl-carnitine; LC-CoA, long-chain acyl-CoA; C, carbon number.

DISCUSSION

Our data show that acyl-CoAs are poorly available for β-oxidation in muscle if they have not been synthesized by ACSL1 (Fig. 7). Endurance exercise in *Acsl1*$^{M-/-}$ mice caused a marked increase in muscle content of long-chain acyl-CoAs. These acyl-CoAs, generated by other ACSL isoforms, were not in a pool that was accessible to the multiprotein CPT1-voltage-dependent anion channel-ACSL1 complex (38,39), and could not be converted to acyl-carnitines or enter the mitochondrial matrix. Thus, acyl-CoAs are located in separate and distinct pools within the cell. This is a surprising result, because amphipathic long-chain acyl-CoAs are water soluble and can interact with membranes and with lipid binding proteins that should allow them to move freely within cells.

Because exercise-activated AMPK downregulates lipid synthesis, lipid synthetic enzymes were apparently unable to handle the excess FA that enters muscle during endurance exercise. Exercise also enhances lipolysis (18,40). Consistent with its critical importance in facilitating acyl-CoA entry into mitochondria and in concert with other peroxisome proliferator–activated receptor α targets, *Acsl1* was the only *Acsl* mRNA upregulated by endurance exercise in control mice (41,42). No change in expression of other *Acsl* isoforms was observed in *Acsl1*$^{M-/-}$ muscle, but exercise increased the low basal specific activity of ACSL in gastrocnemius muscle by 166%, suggesting possible post-transcriptional activation.

A second important finding was that the inability of skeletal muscle to oxidize FA made *Acsl1*$^{M-/-}$ mice vulnerable to systemic hypoglycemia. The dependence of

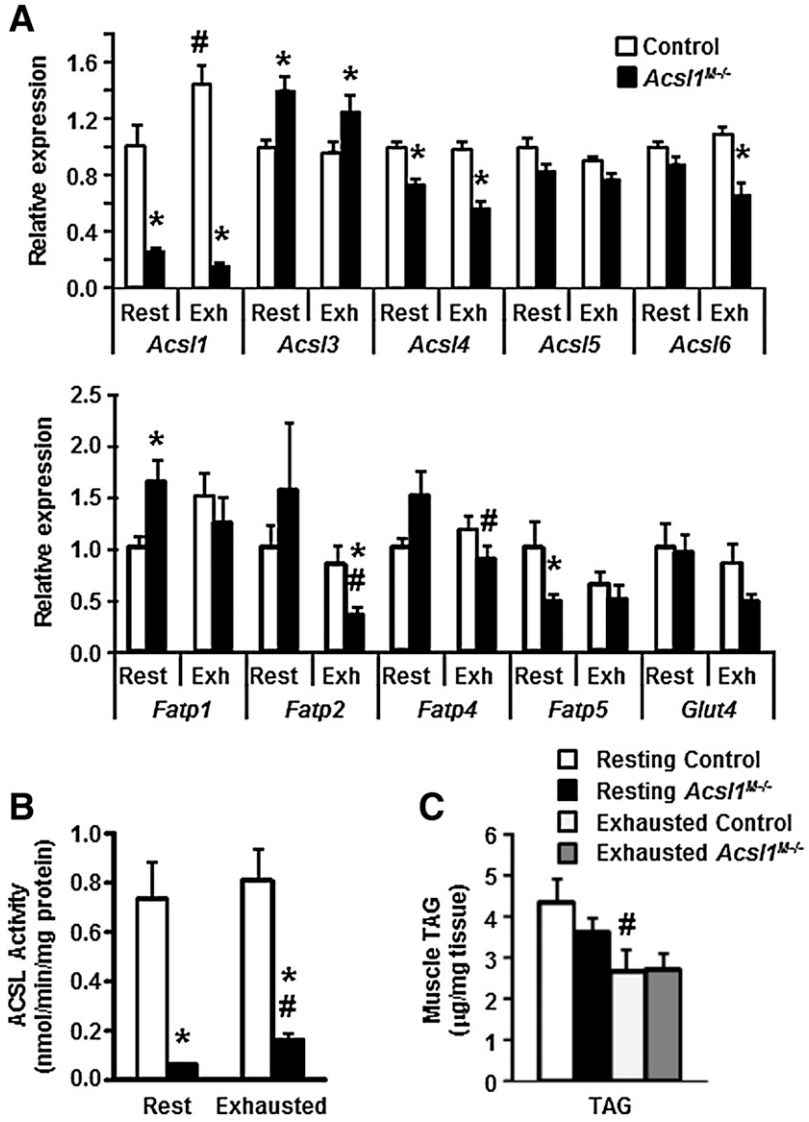

Figure 6— Muscle ACSL1 regulates fuel use and whole-body metabolism. *A*: mRNA expression of *Acsl* isoforms in gastrocnemius muscle relative to tubulin (female, n = 7–9). *B*: ACSL-specific activity within gastrocnemius homogenates (n = 4). *C*: Intramuscular TAG in gastrocnemius muscle after endurance exercise (n = 6–8). #$P < 0.05$, vs. 4-h state (same genotype); *$P < 0.05$, vs. control (same treatment). Exh, exhausted; Rest, resting.

$Acsl1^{M-/-}$ muscle on glucose limited glucose availability for other tissues, and gluconeogenesis was unable to supply sufficient glucose during fasting or exercise. The metabolic profile observed is consistent with muscle that is unable to oxidize FA and, instead, uses hydrolyzed amino acids for energy rather than releasing them as substrates for hepatic gluconeogenesis. Thus, $Acsl1^{M-/-}$ muscle burned more glucose during exercise, and its demand for nonlipid fuel impaired systemic energy homeostasis. The increased demand for glucose during an overnight fast was accompanied by increased muscle GLUT1 protein and enhanced insulin sensitivity in both the liver and muscle.

The marked decrease in FA β-oxidation in $Acsl1^{M-/-}$ muscle resulted in a fasting phenotype of hypoglycemia, elevated plasma FA levels, and fatty liver similar to that of humans and animals with genetic defects in FA oxidation (43,44). However, $Acsl1^{M-/-}$ mice differed from other models of defective FA oxidation in that muscle TAG did not accumulate. Further, because the liver retained normal ACSL activity, fasting-induced hypoketonemic hypoglycemia did not occur (43).

Metabolic limitations on endurance exercise have been variously attributed to low intramuscular fuel stores (45), diminished liver glycogen stores (41), lack of glucose or ketone production by the liver (43), or an impaired ability of muscle to take up and oxidize available fuels, including glucose (46) and FA (43). Diminished endurance in rats is associated with hypoglycemia (45) and with low glycogen content in discrete cerebral regions (47), which may contribute to exhaustion (48).

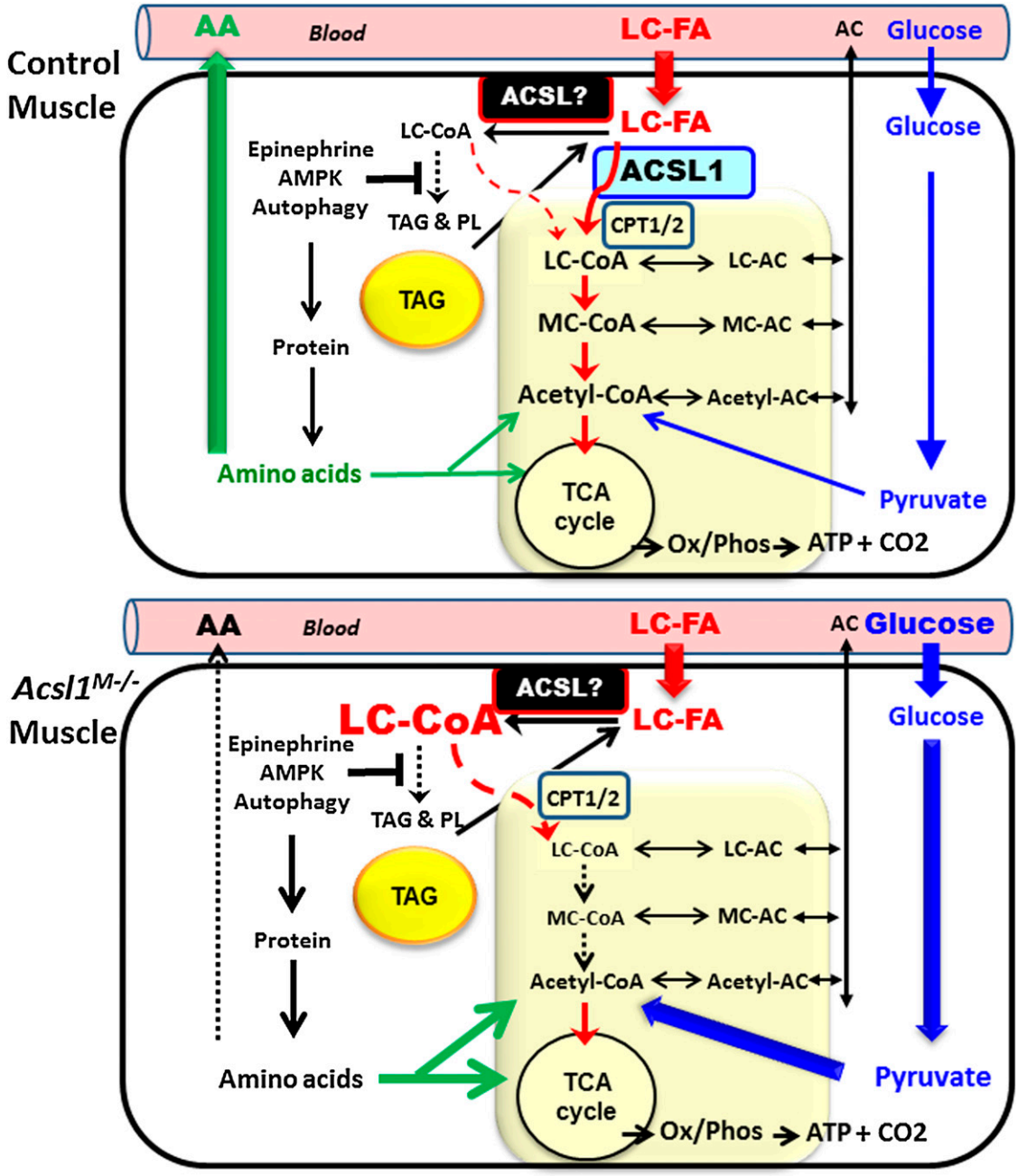

Figure 7—Skeletal muscle metabolism in control and *Acsl1*$^{M-/-}$ mice. *Exercising control muscle*. Initial fuels include glucose hydrolyzed from hepatic and muscle glycogen and intramuscular TAG. Activation of AMPK suppresses TAG synthesis and accelerates mitochondrial FA oxidation, and autophagy releases amino acids, which are exported to provide a substrate for hepatic gluconeogenesis (37). As exercise continues, *Acsl1* mRNA increases, and epinephrine increases the supply of adipocyte-derived long-chain (LC)-FA, which are activated by ACSL1 and converted to LC-acyl-carnitines (ACs) by CPT1 and, within the mitochondria, back to LC-CoA by CPT2. Mitochondrial oxidation produces shorter-chain acyl-CoAs and their AC counterparts. Some amino acids that arise from protein hydrolysis contribute to TCA cycle intermediates and to acetyl-CoA for energy production. Hepatic glucose, now derived via amino acid–fueled gluconeogenesis, continues to enter the glycolytic pathway, but the use of LC-FA spares muscle demand for glucose. In addition to ACs of different chain lengths that move out of the mitochondria into the cytosol, ACs derived from hepatic FA oxidation are released into the blood and equilibrate across the muscle plasma membrane. *Exercising Acsl1*$^{M-/-}$ *muscle*. When ACSL1 is absent, other ACSL isoforms (ACSL?) activate the large amount of entering LC-FA. Most, but perhaps not all, of the LC-CoA produced by these ACSL? lack ready access to CPT1 and cannot be converted to LC-AC and enter the mitochondria. (For simplicity, we have not shown a theoretical pathway by which some FAs might be activated by ACSL? and oxidized in the absence of ACSL1 [see Fig. 1*D*]; these pathways *1*) might provide some LC-CoA at the mitochondrial surface with access to CPT1 or *2*) might provide medium-chain (MC)-CoA in *Acsl1*$^{M-/-}$ muscle [Supplementary Fig. 4*A*], which can enter the mitochondria without CPT1.) The cell content of LC-CoAs increases because of their diminished entry into both oxidative and synthetic pathways. Failure to switch to the use of LC-FA for oxidation enhances glucose entry and oxidation and increases the use of muscle protein–derived amino acid that is converted to acetyl-CoA and TCA cycle intermediates. Fewer amino acids are released by muscle to supply the substrate for hepatic gluconeogenesis. As a consequence, systemic hypoglycemia ensues and the capacity for endurance exercise is impaired.

Failure of muscle to switch to FA use rendered *Acsl1*$^{M-/-}$ mice unable to run optimally, despite normal hepatic FA oxidation and comparable upregulation of mRNA for hepatic gluconeogenic genes. Although a mild myopathy was present, the most striking difference between the running genotypes was the concentration of plasma glucose. *Acsl1*$^{M-/-}$ mice refused to run when their glucose concentrations dropped to ~40 mg/dL, while the controls, with glucose concentrations of ~90 mg/dL, continued to run, despite levels of liver and muscle glycogen, muscle TAG, and plasma ketones, FA, and amino acids equivalent to those of the knockouts. Thus, hypoglycemia, causing central fatigue and an inadequate peripheral energy supply, was the deciding feature in the refusal of both genotypes to run.

In summary, ACSL1 is essential for FA oxidation in skeletal muscle, and acyl-CoA synthesis by other ACSL isoforms cannot compensate (Fig. 7). ACSL1 is located on both the endoplasmic reticulum and the mitochondrial outer membrane in rat liver (38,49) and 3T3-L1 adipocytes (50), but the subcellular location of ACSL1 in muscle has not been investigated. The absence of ACSL1 resulted in an inappropriate dependence on glucose for muscle energy, such that systemic glucose homeostasis became severely compromised. In human and animal models with defective FA oxidation, the hypoglycemia that occurs with fasting or exercise has been attributed to a lack of hepatic FA metabolism and diminished ATP production to power gluconeogenesis. In *Acsl1*$^{M-/-}$ mice, however, hypoglycemia occurred despite the fact that hepatic FA oxidation was not impaired. Instead, the muscle-specific defect in FA oxidation drained the glucose supply, and the likely increased use of amino acids within muscle precluded amino acid availability as a substrate for hepatic gluconeogenesis. Thus, during both fasting and endurance exercise, the liver was unable to synthesize sufficient glucose to prevent hypoglycemia, a dramatic example of the interdependence of muscle and liver fuel metabolism.

Funding. This work was supported by National Institutes of Health grants T32HL069768 (T.J.G.), DK058398 (C.B.N.), AG028930 (D.M.M.), and DK59935 and DK59935(ARRA) (R.A.C.); the UNC Nutrition Obesity Research Center grant P30DK56350; and Ellison Medical Foundation grant AG-NS-0548-09 (T.R.K.).

Duality of Interest. No potential conflicts of interest relevant to this article were reported.

Author Contributions. L.O.L. designed and performed the research, wrote the manuscript, and contributed to the writing of the final submitted version of the manuscript. T.J.G., D.S.P., T.R.K., and F.P. performed the research and contributed to the writing of the final submitted version of the manuscript. O.I. performed the research. C.B.N. and D.M.M. contributed to the writing of the final submitted version of the manuscript. R.A.C. designed the research, wrote the manuscript, and contributed to the writing of the final submitted version of the manuscript. R.A.C. is the guarantor of this work and, as such, had full access to all the data in the study and takes responsibility for the integrity of the data and the accuracy of the data analysis.

References

1. Kelley DE, Mandarino LJ. Fuel selection in human skeletal muscle in insulin resistance: a reexamination. Diabetes 2000;49:677–683
2. Thyfault JP, Rector RS, Noland RC. Metabolic inflexibility in skeletal muscle: a prelude to the cardiometabolic syndrome? J Cardiometab Syndr 2006;1:184–189
3. Watt MJ, Hoy AJ. Lipid metabolism in skeletal muscle: generation of adaptive and maladaptive intracellular signals for cellular function. Am J Physiol Endocrinol Metab 2012;302:E1315–E1328
4. Zhang D, Liu ZX, Choi CS, et al. Mitochondrial dysfunction due to long-chain Acyl-CoA dehydrogenase deficiency causes hepatic steatosis and hepatic insulin resistance. Proc Natl Acad Sci USA 2007;104:17075–17080
5. Ukropcova B, Sereda O, de Jonge L, et al. Family history of diabetes links impaired substrate switching and reduced mitochondrial content in skeletal muscle. Diabetes 2007;56:720–727
6. Sahlin K, Harris RC. Control of lipid oxidation during exercise: role of energy state and mitochondrial factors. Acta Physiol (Oxf) 2008;194:283–291
7. Jeppesen J, Jordy AB, Sjøberg KA, et al. Enhanced fatty acid oxidation and FATP4 protein expression after endurance exercise training in human skeletal muscle. PLoS One 2012;7:e29391
8. Baruteau J, Sachs P, Broué P, et al. Clinical and biological features at diagnosis in mitochondrial fatty acid beta-oxidation defects: a French pediatric study of 187 patients. J Inherit Metab Dis 2013;36:795–803
9. Holloszy JO, Kohrt WM. Regulation of carbohydrate and fat metabolism during and after exercise. Annu Rev Nutr 1996;16:121–138
10. Ellis JM, Frahm JL, Li LO, Coleman RA. Acyl-coenzyme A synthetases in metabolic control. Curr Opin Lipidol 2010;21:212–217
11. Li LO, Klett EL, Coleman RA. Acyl-CoA synthesis, lipid metabolism and lipotoxicity. Biochim Biophys Acta 2010;1801:246–251
12. Li LO, Ellis JM, Paich HA, et al. Liver-specific loss of long chain acyl-CoA synthetase-1 decreases triacylglycerol synthesis and beta-oxidation and alters phospholipid fatty acid composition. J Biol Chem 2009;284:27816–27826
13. Ellis JM, Li LO, Wu PC, et al. Adipose acyl-CoA synthetase-1 directs fatty acids toward beta-oxidation and is required for cold thermogenesis. Cell Metab 2010;12:53–64
14. Ellis JM, Mentock SM, Depetrillo MA, et al. Mouse cardiac acyl coenzyme a synthetase 1 deficiency impairs fatty acid oxidation and induces cardiac hypertrophy. Mol Cell Biol 2011;31:1252–1262
15. Watt MJ, Hoy AJ, Muoio DM, Coleman RA. Distinct roles of specific fatty acids in cellular processes: implications for interpreting and reporting experiments. Am J Physiol Endocrinol Metab 2012;302:E1–E3
16. Schwander M, Leu M, Stumm M, et al. Beta1 integrins regulate myoblast fusion and sarcomere assembly. Dev Cell 2003;4:673–685
17. Leonardi R, Rehg JE, Rock CO, Jackowski S. Pantothenate kinase 1 is required to support the metabolic transition from the fed to the fasted state. PLoS One 2010;5:e11107
18. Kiens B. Skeletal muscle lipid metabolism in exercise and insulin resistance. Physiol Rev 2006;86:205–243
19. Passonneau JV, Lauderdale VR. A comparison of three methods of glycogen measurement in tissues. Anal Biochem 1974;60:405–412
20. Wendel AA, Li LO, Li Y, Cline GW, Shulman GI, Coleman RA. Glycerol-3-phosphate acyltransferase 1 deficiency in ob/ob mice diminishes hepatic steatosis but does not protect against insulin resistance or obesity. Diabetes 2010;59:1321–1329
21. Folch J, Lees M, Sloane Stanley GH. A simple method for the isolation and purification of total lipides from animal tissues. J Biol Chem 1957;226:497–509
22. Engel AG, Franzini-Armstrong C. *Myology*: *Basic and Clinical*. New York, McGraw-Hill, 2004
23. Livak KJ, Schmittgen TD. Analysis of relative gene expression data using real-time quantitative PCR and the 2(-Delta Delta C(T)) method. Methods 2001;25:402–408
24. Polokoff MA, Bell RM. Limited palmitoyl-CoA penetration into microsomal vesicles as evidenced by a highly latent ethanol acyltransferase activity. J Biol Chem 1978;253:7173–7178
25. Noland RC, Woodlief TL, Whitfield BR, et al. Peroxisomal-mitochondrial oxidation in a rodent model of obesity-associated insulin resistance. Am J Physiol Endocrinol Metab 2007;293:E986–E1001

26. Ferrara CT, Wang P, Neto EC, et al. Genetic networks of liver metabolism revealed by integration of metabolic and transcriptional profiling. PLoS Genet 2008;4:e1000034
27. An J, Muoio DM, Shiota M, et al. Hepatic expression of malonyl-CoA decarboxylase reverses muscle, liver and whole-animal insulin resistance. Nat Med 2004;10:268–274
28. Muoio DM, Noland RC, Kovalik JP, et al. Muscle-specific deletion of carnitine acetyltransferase compromises glucose tolerance and metabolic flexibility. Cell Metab 2012;15:764–777
29. Kersten S, Seydoux J, Peters JM, Gonzalez FJ, Desvergne B, Wahli W. Peroxisome proliferator-activated receptor alpha mediates the adaptive response to fasting. J Clin Invest 1999;103:1489–1498
30. van Ginneken V, Verhey E, Poelmann R, et al. Metabolomics (liver and blood profiling) in a mouse model in response to fasting: a study of hepatic steatosis. Biochim Biophys Acta 2007;1771:1263–1270
31. Frayn KN. Fat as a fuel: emerging understanding of the adipose tissue-skeletal muscle axis. Acta Physiol (Oxf) 2010;199:509–518
32. Stellingwerff T, Boon H, Jonkers RA, et al. Significant intramyocellular lipid use during prolonged cycling in endurance-trained males as assessed by three different methodologies. Am J Physiol Endocrinol Metab 2007;292:E1715–E1723
33. Watkins PA. Very-long-chain acyl-CoA synthetases. J Biol Chem 2008;283: 1773–1777
34. Westin MA, Hunt MC, Alexson SE. Short- and medium-chain carnitine acyltransferases and acyl-CoA thioesterases in mouse provide complementary systems for transport of beta-oxidation products out of peroxisomes. Cell Mol Life Sci 2008;65:982–990
35. Rennie MJ, Tipton KD. Protein and amino acid metabolism during and after exercise and the effects of nutrition. Annu Rev Nutr 2000;20:457–483
36. He C, Bassik MC, Moresi V, et al. Exercise-induced BCL2-regulated autophagy is required for muscle glucose homeostasis. Nature 2012;481:511–515
37. Dohm GL, Tapscott EB, Kasperek GJ. Protein degradation during endurance exercise and recovery. Med Sci Sports Exerc 1987;19(Suppl.):S166–S171
38. Lee K, Kerner J, Hoppel CL. Mitochondrial carnitine palmitoyltransferase 1a (CPT1a) is part of an outer membrane fatty acid transfer complex. J Biol Chem 2011;286:25655–25662
39. Alfonso-Pecchio A, Garcia M, Leonardi R, Jackowski S. Compartmentalization of mammalian pantothenate kinases. PLoS One 2012;7:e49509
40. Steinberg GR. Role of the AMP-activated protein kinase in regulating fatty acid metabolism during exercise. Appl Physiol Nutr Metab 2009;34:315–322
41. Muoio DM, MacLean PS, Lang DB, et al. Fatty acid homeostasis and induction of lipid regulatory genes in skeletal muscles of peroxisome proliferator-activated receptor (PPAR) alpha knock-out mice. Evidence for compensatory regulation by PPAR delta. J Biol Chem 2002;277:26089–26097
42. Martin G, Schoonjans K, Lefebvre AM, Staels B, Auwerx J. Coordinate regulation of the expression of the fatty acid transport protein and acyl-CoA synthetase genes by PPARalpha and PPARgamma activators. J Biol Chem 1997; 272:28210–28217
43. Spiekerkoetter U, Wood PA. Mitochondrial fatty acid oxidation disorders: pathophysiological studies in mouse models. J Inherit Metab Dis 2010;33:539–546
44. Wanders RJ, Vreken P, den Boer ME, Wijburg FA, van Gennip AH, IJlst L. Disorders of mitochondrial fatty acyl-CoA beta-oxidation. J Inherit Metab Dis 1999;22:442–487
45. Winder WW, Yang HT, Jaussi AW, Hopkins CR. Epinephrine, glucose, and lactate infusion in exercising adrenodemedullated rats. J Appl Physiol (1985) 1987;62:1442–1447
46. MacLean PS, Zheng D, Dohm GL. Muscle glucose transporter (GLUT 4) gene expression during exercise. Exerc Sport Sci Rev 2000;28:148–152
47. Matsui T, Soya S, Okamoto M, Ichitani Y, Kawanaka K, Soya H. Brain glycogen decreases during prolonged exercise. J Physiol 2011;589:3383–3393
48. Nybo L, Secher NH. Cerebral perturbations provoked by prolonged exercise. Prog Neurobiol 2004;72:223–261
49. Lewin TM, Kim JH, Granger DA, Vance JE, Coleman RA. Acyl-CoA synthetase isoforms 1, 4, and 5 are present in different subcellular membranes in rat liver and can be inhibited independently. J Biol Chem 2001;276:24674–24679
50. Gargiulo CE, Stuhlsatz-Krouper SM, Schaffer JE. Localization of adipocyte long-chain fatty acyl-CoA synthetase at the plasma membrane. J Lipid Res 1999; 40:881–892